SELECTION OF VARIABLE GAIN SETTINGS FOR IRS- P6: LISS SENSORS

V. Srinivas, S. Muralikrishnan A. Senthil Kumar*

Data Processing Area, National Remote Sensing Agency, Balanagar, Hyderabad 500 037 INDIA.
(muralikrishnan_s, senthilkumar_a)@nrsa.gov.in

Commission IV, WG-IV/10

KEY WORDS: Signal-to-noise ratio, Spectral radiance, Relative spectral response, Saturation radiance, sensor linear response.

ABSTRACT

IRS-P6 spacecraft provides a unique opportunity of acquiring simultaneously multispectral (MS) data in three different spatial resolutions at 5.8 m, 23.5 m and 56 m, respectively, from LISS-4, LISS-3 and AWIFS sensors. Of these, spectral bands of the AWIFS (excepting the MIR band) have been designed to cover a 100% albedo, and with 10 bits per pixel to provide a good distribution of grey values for almost ground features. The LISS-3 and LISS-4 sensors have been designed with variable electronic gain settings, much similar to the LANDSAT-TM and SPOT HRV sensors, in order to cover the scene reflectance within the linear dynamic range of the sensors. Given the gain settings (equivalently Saturation Radiance, SR) permitted onboard for the LISS sensors, a study was conducted to select appropriate sets of gain values applicable to different terrain features and solar illumination conditions. In this paper, we describe the method followed, based upon experiments with the AWIFS data acquired specifically to cover terrain features and theoretical approaches for computing the top-of-atmosphere radiances for these features. Selection of the SR is to be chosen based on application requirements. The SR value larger than the optimum would result the terrain feature of interest covering only a small portion of the dynamic range of the output. On the other hand, if it is set at a lower value, then many common terrain features in the image would saturate, thereby limiting the data usability. Also, as the at-sensor radiance is dependent nonlinearly on the solar incident angle at the given scene, it is essential to take into account of the influence by the solar incident angle, which varies significantly for two major seasons in a year. The required data collected over cities, deserts, vegetation, lakes etc., across the globe were used here. Radiometric model of IRS MS sensors was described first, and a method of evaluating expected probable maximum spectral radiance for each feature of interest was given. Theoretical and experimental results obtained were compared to arrive operable gain settings appropriate for global data usage of IRS-P6 LISS data.

1. Introduction

The IRS-P6 (also known as IRS-Resourcesat-1) satellite, launched in late 2003, provides a unique opportunity of acquiring simultaneously multispectral (MS) data in three different spatial resolutions from three independent optical sensors, namely, (i) LISS-3 (B2: 0.52 – 0.59 μm; B3: 0.62 – 0.68 μm; B4: 0.77 – 0.86 μm; B5: 1.55 – 1.70 μm) at a ground resolution of 24 m covering a swath of 141 km, (ii) an Advanced Wide Field Sensor (AWIFS) at a ground resolution of 56 m and swath of 760 km in same spectral bands as of the LISS-3 and (iii) LISS-4 sensor operating in B2, B3 and B4 spectral bands of LISS-3 at a ground resolution of 5 m (NRSA, 2003). The satellite data can be acquired in both real-time overpass covering the terrain area within the visibility limit of its ground reception stations, or play-back mode by recording the data acquired elsewhere with the help of solid state recorder (capacity: 120 GB) and by dumping the data when the satellite traverses over its ground stations distributed across the globe.

Of these three sensors, spectral bands of the AWIFS (excepting the MIR band) have been designed to cover a 100% albedo, and with 10 bits per pixel to provide a good distribution of gray values for almost ground features. The LISS-3 and LISS-4 sensors have been designed with variable electronic gain settings, much similar to the LANDSAT-TM and SPOT HRV sensors, in order to cover the scene reflectance within the linear dynamic range of the sensors. Given the gain settings permitted onboard for the LISS sensors, a study was conducted to select appropriate sets of gain values applicable to different terrain features and solar illumination conditions. In this paper, we describe the method followed, based upon experiments with the AWIFS data acquired specifically to cover terrain features and theoretical approaches for computing the top-of-atmosphere radiances for these features.

The rest of the paper is organized as follows: First, radiometric model followed by IRS electro-optical sensors is described. Second, methodologies used for computing maximum probable radiances to be received at the sensor onboard were given. Third, results obtained from the AWIFS data and from theoretical approach were given in order to arrive at a set of gain settings for the LISS-3 and LISS-4 sensors. Our conclusions are discussed in Sec. 5.

2. Radiometric model for IRS sensors

The solar light from the Earth feature, reflected and passed by the IRS-LISS band *k*, is first converted to photo-electric signal by charge coupled device and further amplified electronically by a factor of G_m, before it is converted into a digital raw data (referred to as Level-0 for IRS product). This raw data can be related to top-of-atmosphere (TOA) spectral radiance by

$$V_{jk} = G_m \, g_{jk} \, L_k + c_{jk} \qquad (1)$$

Here, parameters (g_{jk}, c_{jk}) denote, respectively, the relative gain and offset values of detector *j*, and m ∈ [1, 4]. Depending on the choice of G_m, the raw digital number (DN) can reach a maximum value, $DN_{\max}$ (=127, for 7 bit

* Corresponding author

raw data for the LISS-3 and LISS-4), which, in turn, results in saturation radiance (SR) given by

$$SR_{jk} = \frac{127 - c_{jk}}{g_{jk}\, G_m}. \qquad (2)$$

The dependence of SR on detector *j* is removed during the radiometric normalization step, in which outputs of all the detectors are made to map to the one detector (the one reaching fastest to saturation) taken as reference *r*. The reference detector should ideally have its normalization coefficients: $g_r = 1.0$ count per unit radiance and $c_r = 0$ count. Since all the higher levels of LISS data products are supplied with 8 bits per pixel, g_r value is set to 0.5 to stretch the raw digital count, and processed without truncating till the final levels of products are generated. The radiometrically normalized digital number, DN_k^N is related to spectral radiance for band *k* by the relation

$$L_k(m,n) = \frac{DN_k^N(m,n) \cdot SR_k}{DN_{\max}} \qquad (3)$$

Selection of the SR or equivalently the gain setting is to be chosen based on application requirements. If a large SR value is chosen more than an optimum, the DN range that the terrain feature of user interest may cover only a small portion of the dynamic range of the output. On the other hand, it is chosen than the optimum, then many common terrain features may saturate, thereby limiting the data usability. Table 1 gives the saturation radiances chosen at different operable gain settings for the IRS-P6 sensors. As the at-sensor radiance is dependent nonlinearly on the solar incident angle at the given scene, it is essential to take into account of the influence by the solar incident angle, which varies significantly for two major seasons in a year.

Table 1 Saturation Radiances at different gain settings of P6: MS sensors.

Sensor/ Band	Spectral range (μm)	SR (mW/cm^2-sr-μm) G1	G2	G3	G4	E_0 (mW/ /cm^2-μm)
LISS-3						
B2	0.52 – 0.59	26.6	18.5	12.1	8.9	184.95
B3	0.63 – 0.69	27.3	18.2	15.1	10.3	155.30
B4	0.77 – 0.86	31.0	20.7	15.8	10.9	109.20
B5	1.55 – 1.70	6.9	3.4	1.6	0.8	23.95
LISS-4						
B2	0.52 – 0.59	58.2	27.2	11.6	3.6	185.36
B3	0.63 – 0.69	46.4	23.1	9.9	3.8	158.36
B4	0.77 – 0.86	36.8	17.2	7.4	2.3	111.43
AWIFS						
B2	0.52 – 0.59	52.34	–	–	–	185.47
B3	0.63 – 0.69	40.75	–	–	–	155.68
B4	0.77 – 0.86	28.42	–	–	–	108.27
B5	1.55 – 1.70	4.64	–	–	–	23.98

3. Estimation of Saturation Radiance

As mentioned earlier, the IRS AWIFS could provide spectral radiance values for almost all the features (excepting thick clouds) without data saturation. The required data collected over cities, deserts, vegetation, lakes etc., across the globe were used here. Due to dependence of TOA radiance on the solar incident angle, the data were chosen to cover a wide range of latitudes and obtained different times of the year.

Following procedure was adapted to compute the SR from the AWIFS data.

1) Select visually a small window to get homogeneous signature of the terrain feature under study. In our case, it was found sufficient to choose a (5 x 5) image window for most features of interest. The maximum radiance $L_{k\max}$ and its standard deviation (σ_k) are first obtained, following by the DN-to-radiometric formula given in the data product header. These values are then used to calculate the probable maximum spectral radiance (PMSR) (Sharma and Medhavy, 1994):

$$\text{PMSR} = L_{k\max} + 3\,\sigma_k \qquad (4)$$

2) As mentioned above, the at-sensor radiance is dependent nonlinearly on the solar incident angle. From a large number of data sets analyzed in the northern hemisphere, it was found appropriate to compute the SR for solar elevation angle of 70° for summer (April - September) and 45° for fall (October – March) seasonal conditions. The saturation radiances for the selected feature is then estimated by normalizing the solar incident angle on the scene to the above maximum angles as, respectively,

$$L_{max} = PMSR * \frac{\sin 70^\circ}{\sin \theta_{ele}}, \quad \text{and}$$

$$L_{\max} = PMSR * \frac{\sin 45^\circ}{\sin \theta_{ele}} \qquad (5)$$

as applicable for the summer and fall seasons in the northern hemisphere part of the globe, and vice-versa for southern hemisphere regions during these periods. Variation due to sensor spectral response within pass-band between the AWIFS to the LISS-3 and LISS-4 for a given band is to be accounted. A normalizing factor M was computed from the response curves of LISS and AWIFS of band *i*, with ($-\infty < \lambda < +\infty$), as:

a.

$$M_{Li} = \frac{\int S_{Li}(\lambda)\, d\lambda}{\int S_{AWi}(\lambda)\, d\lambda} \qquad (6)$$

Even though the integrand extends for the entire spectrum, it has been observed from the RSR values, each band was characterized by a high transmittance zone within the pass-band, and having of a steep rise and sharp fall within the spectral range. In our study, a threshold of about 10% was set to eliminate the non-significant spectral range of the RSR to compute the normalizing factor between corresponding bands of the LISS-3 and LISS-4 with the AWIFS.

To compute theoretically, the TOA spectral radiance at the sensor must be estimated. The TOA spectral radiance of a given feature is given by well-known radiation formula:

$$L_k = \frac{E_{0k} \cos\theta_z}{\pi\, d_s}\, \rho_k \tau + L_p \qquad (7)$$

where E_k is the exo-atmospheric solar irradiance in spectral band *k*, θ_z, the solar zenith angle, and d_s is the Earth – Sun distance in Astronomical units, τ, the atmospheric transmittance, ρ_k, the feature spectral reflectance within the pass-band of band *k*, and L_p, the atmospheric path radiance which accounts both the sky and

background radiances. The values of E_k was dependent on wavelength of incident radiation and the RSR. The computed E_k for each LISS spectral bands following the procedure given in (Pandya et al., 2002) and are given in Table 1. The path radiance depends on many factors, e.g., viewing geometry, wavelength of incident light, aerosol content of the atmosphere etc., and is generally derived from a radiative transfer model. Montgomery et al. (1990) have reported both the L_k and L_p at 15 wavelengths ranging from 0.4 μm to 2.25 μm for sun zenith angles ranging from 0 to 80 degrees. The input parameters used in their study included vertical profiles, absorption and scattering optical thicknesses of particulates (gases and aerosols) for about 10 surface reflectance values. Earlier, Bowker et al. (1985) reported a catalog of laboratory-measured reflectance curves for various surface targets. These reflectance values were used to compute the TOA spectral radiance for two sun angles within each spectral band, taking into account on the spectral filter pass-band from the RSR.

4. Results and Discussions

Simulated spectral radiances of LISS-3 from the AWIFS data for different ground features are shown as a function of band number in Figure 1. For comparison, the radiance computed theoretically was also plotted. Even though, the trend of radiance variation with band number remains from both the methods, there are deviations noticeable, especially in the visible-near IR bands. In the case of sand, for e.g., theoretical radiance value was higher than the simulated LISS-3 radiance for B2, but lower for B3 and B4. On the other hand, theoretical radiance for vegetation is higher for B2 and B3 and lower for B4. It should be noted that both the methods yield very similar values for B5 spectral band. The reason for this can be attributed to the prediction of path radiance in the theoretical approach. Of course, this can be attributed to error in absolute calibration of the IR sensor output. This is, however, unlikely due to the fact that light sources used in the pre-flight calibration of the IRS sensors are traceable to sources of NIST standard, and accuracy in absolute radiance is known to be better than 5%. An average plot of the radiances is shown in Figure 3. Inferences from the study for land cover features, covering low, middle and high reflectance regions are as given below:

Vegetation: This being the prime target of importance for the RESOURCESAT-1 mission, it is important that this feature class should not be allowed to be saturated in all bands, and gain settings are such that good contrast is met for discriminating discrete species and textural information. The vegetation cover radiances, normalized to sun angle of 20°, observed over different parts of the globe are shown in Fig. 2a.

Desert Sand: This feature is of great importance for absolute and inter-sensor calibration exercises. Since this feature in general spreads across a large area and assumes flat signature, the data acquired over this helps in post-launch correction of relative photo-response variations across the detector array. The radiances observed for desert sand features across the globe at various sites targeted for vicarious calibration are shown in Fig. 2b.

Urban: The urban scenes are especially demanded from LISS-4 MX sensor due to its wider swath of 23 km – a feature not available with other very high resolution MS commercial sensors. This coverage is of importance for urban sprawl and settlement related analysis. The normalized radiances observed at urban environs are shown in Fig. 2c. It should be noted that radiance of the urban cover in desert environ is higher than the typical urban environ. This observation holds good for other features; it is thus important to treat desert environs as separate domain from the normal urban environ.

Figure 2 Simulated spectral radiances of LISS-3 for (a) vegetation, (b) desert sand and (c) urban features across different locations in the globe.

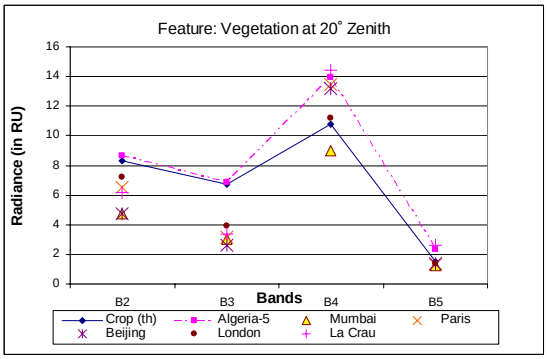

(a)

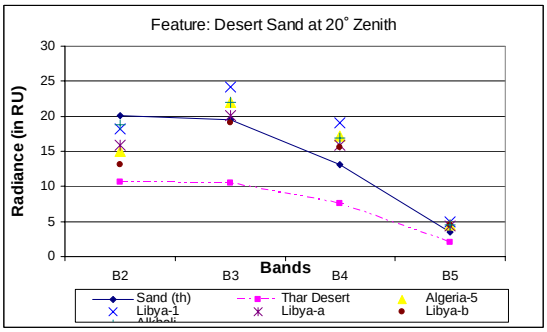

(b)

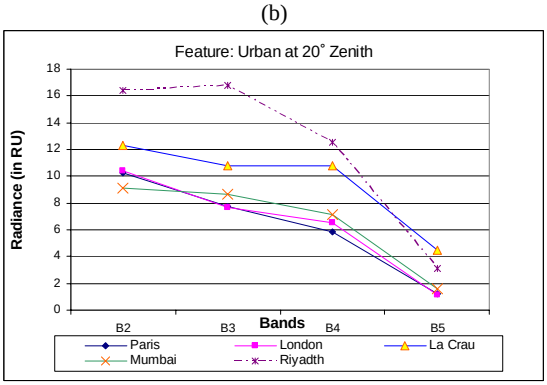

(c)

Table 2 gives required radiance limits from the simulated PMSR values at LISS-3 spectral bands for sun angles of (a) 20° and (b) 45° respectively for some features of user interest from the northern hemisphere. As mentioned earlier, the values are changed vice versa for the southern hemisphere. Even though there would be small variations for these features for southern hemisphere, these were much less than 10% and, hence were ignored.

Table 2 Required LISS-3 Radiances for sun angles of (a) 20° and (b) 45°, for different land cover features in the northern hemisphere.

Features	B2	B3	B4	B5
Urban Environ				
City	> 13	> 12	> 12	> 6
Dry Soil	> 10	> 9.6	> 9	> 3
Vegetation	> 8	> 5	> 12	> 2
Cloud	> 28	> 25	> 20	> 5
Water	> 6	> 3	> 2	> 1
Salt Pan	> 24	> 23	> 15	> 1.5
Desert Environ				
City	> 17	> 17	> 13	> 7
Sand	> 20	>25	> 20	>5
Vegetation	> 10	> 7	> 15	> 3
Cloud	> 27	> 29	> 21	> 5
Water	> 7	>6.5	>5.2	>1.4

(a)

Features	B2	B3	B4	B5
Urban Environ				
City	> 8	> 7	> 6	> 2
Dry soil	> 8	> 7	> 7	> 2
Vegetation	> 5	> 3	> 9	> 2
Cloud	> 21	> 19	> 15	> 3
Water	> 5	> 3	> 2	> 1
Salt Pan	> 18	> 17	> 11	> 1
Desert Environ				
City	>12	>13	>10	>3
Sand	>13	>15	>12	> 4
Vegetation	> 6	> 5	> 11	> 2
Cloud	> 21	> 22	> 16	> 3
Water	> 5	> 5	> 4	> 2

(b)

Table 3 Suggested global Gain settings (SRs) for P6: LISS-3 Sensors as applicable for (a) April-September and (b) October-March period of months.

April-September				
N. Hemisphere	**B2**	**B3**	**B4**	**B5**
Urban Environ	G2 (18.5)	G2 (18.2)	G2 (20.7)	G2 (3.4)
Desert Environ	G1 (26.6)	G1 (27.3)	G2 (20.7)	G1 (6.9)
S. Hemisphere	**B2**	**B3**	**B4**	**B5**
Urban Environ	G3 (12.1)	G3 (15.1)	G3 (15.8)	G2 (1.6)
Desert Environ	G2 ((18.5)	G2 (18.2)	G2 (20.7)	G1 (6.9)

(a)

Oct-March				
N. Hemisphere	**B2**	**B3**	**B4**	**B5**
Urban Environ	G3 (12.1)	G3 (15.1)	G3 (15.8)	G2 (3.4)
Desert Environ	G2 (18.5)	G2 (18.2)	G2 (20.7)	G1 (6.9)
S. Hemisphere	**B2**	**B3**	**B4**	**B5**
Urban Environ	G2 (18.5)	G2 (18.2)	G2 (20.7)	G2 (3.4)
Desert Environ	G2 (18.5)	G1 (27.3)	G2 (20.7)	G1 (6.9)

(b)

Table 3 gives the suggested gain settings for RESOURCESAT-1: LISS-3. Corresponding saturation radiances of these gain settings are also shown. These values were arrived by comparing the saturation radiances given in Table 1 and required spectral radiances for various ground features given in Table 2. From Table 2a, it can be seen that clouds followed by saltpan had high radiance values, but setting them to these values would reduce the dynamic range of the image data. Considering these and mission objectives, G2 is taken as gain for LISS-3 B2 which would cater all other features of importance within the sensor linear range. Similar exercise was carried out for LISS-4 MX data using its SR values given in Table 1 and spectral radiance requirements for ground targets shown in Table 2.

5. Conclusions

A systematic method of arriving at operable gain settings was suggested based on theoretic knowledge of spectral reflectances and radiometric model of IRS, and normalizing the observed radiances obtained from 10 bit multispectral data from P6 AWIFS sensor. Images from different ground targets across the globe were analysed to derive the suitable gain settings to make the features of high importance to be within the sensor linear range. It was observed that in general, the desert environ features would differ from the typical urban environ and need to be treated as separate case.

REFERENCES

Bowker, D. E., Davis, R. E., Myrick, D.L., Stacy, K and Jones, W.T (1995). Spectral Reflectance of natural targets for use in remote sensing studies, NASA-RP. No.1139.

NRSA., 2003. IRS-P6 data user's handbook. National Remote Sensing Agency, Hyderabad, India. http://www.nrsa.gov.in/engnrsa/p6book/handbook/handbook.pdf

Pandya, M.R. et al., 2002. Band-pass Solar Exo-atmospheric Irradiance and Rayleigh Optical Thickness of Sensor On Board IRS Satellite -1B,1C,1D and P4. IEEE Trans. Geosci. Remote Sensing, vol. 40, No. 13, pp. 714 – 718.

Sharma, T. and Medhavy, T.T. 1994. Procedures for computation of Saturation Radiances. J. Ind. Soc. Remote Sensing, vol. 22, No. 1, pp. 9-19.

Montgomery, H.E., Ostrow, H. and Ressler, G.M. 1990. Sensor Performance Analysis, NASA RP-1241.